



OPEN ACCESS

EDITED BY

Rizwan Ur Rehman Sagar,
Jiangxi University of Science and Technology,
China

REVIEWED BY

Faheem K. Butt,
University of Education Lahore, Pakistan
Hamad Ashraf,
Ruhr University Bochum, Germany

*CORRESPONDENCE

Nadeem Sabir,
✉ nadeemsabir@gcuf.edu.pk
Muhammad Zahid,
✉ rmzahid@uaf.edu.pk

RECEIVED 06 April 2024

ACCEPTED 04 June 2024

PUBLISHED 03 July 2024

CITATION

Shahbaz M, Sabir N, Amin N, Zulfiqar Z and
Zahid M (2024), Synthesis and characterization
of chromium aluminum carbide MAX phases
(Cr_xAlC_{x-1}) for potential
biomedical applications.
Front. Chem. 12:1413253.
doi: 10.3389/fchem.2024.1413253

COPYRIGHT

© 2024 Shahbaz, Sabir, Amin, Zulfiqar and
Zahid. This is an open-access article distributed
under the terms of the [Creative Commons
Attribution License \(CC BY\)](#). The use,
distribution or reproduction in other forums is
permitted, provided the original author(s) and
the copyright owner(s) are credited and that the
original publication in this journal is cited, in
accordance with accepted academic practice.
No use, distribution or reproduction is
permitted which does not comply with these
terms.

Synthesis and characterization of chromium aluminum carbide MAX phases (Cr_xAlC_{x-1}) for potential biomedical applications

Muhammad Shahbaz^{1,2}, Nadeem Sabir^{1*}, Nasir Amin¹,
Zobia Zulfiqar¹ and Muhammad Zahid^{3*}

¹Department of Physics, Govt College University Faisalabad, Faisalabad, Pakistan, ²Punjab Institute of Nuclear Medicine (PINUM), Faisalabad, Pakistan, ³Department of Chemistry, University of Agriculture Faisalabad, Faisalabad, Pakistan

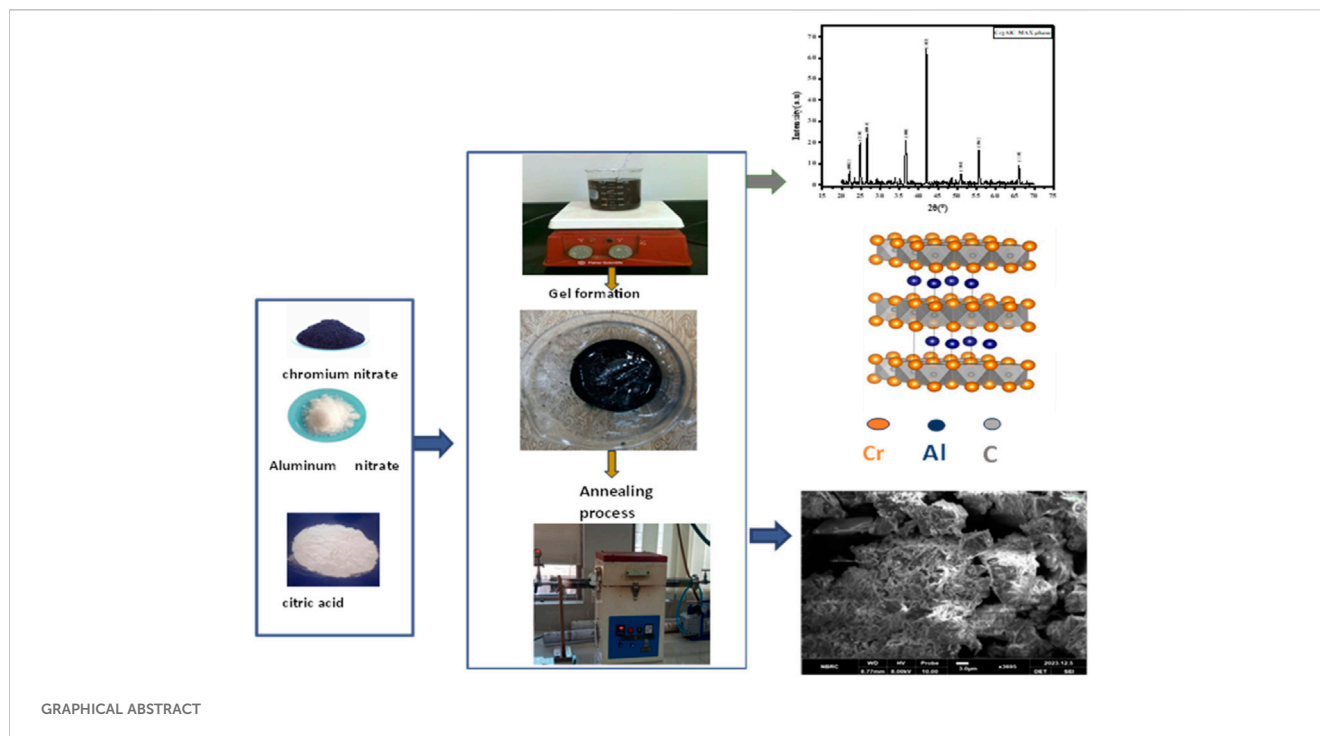
MAX phases, characterized as nanolaminates of ternary carbides/nitrides structure, possess a unique combination of ceramic and metallic properties, rendering them pivotal in materials research. In this study, chromium aluminum carbide ternary compounds, Cr₂AlC (211), Cr₃AlC₂ (312), and Cr₄AlC₃ (413) were successfully synthesized with high purity using a facile and cost-effective sol-gel method. Structural, morphological, and chemical characterization of the synthesized phases was conducted to understand the effects of composition changes and explore potential applications. Comprehensive characterization techniques including XRD for crystalline structure elucidations, SEM for morphological analysis, EDX for chemical composition, Raman spectroscopy for elucidation of vibrational modes, XPS to analyze elemental composition and surface chemistry, and FTIR spectroscopy to ensure the functional groups analysis, were performed. X-ray diffraction analysis indicated the high purity of the synthesized Cr₂AlC phase as well as other ternary compounds Cr₃AlC₂ and Cr₄AlC₃, suggesting its suitability as a precursor for MXenes production. Additionally, the antimicrobial activity against *Candida albicans* and biocompatibility assessments against *Escherichia coli* (*E. coli*), *Staphylococcus aureus* (*S. aureus*), and HepG2 cell line were investigated. The results demonstrated significant antifungal activity of the synthesized phases against *Candida albicans* and negligible impact on the viability of *E. coli* and *S. aureus*. Interestingly, lower concentrations of Cr₂AlC MAX phase induced cytotoxicity in HepG2 cells by triggering intercellular oxidative stress, while Cr₃AlC₂ and Cr₄AlC₃ exhibited lower cytotoxicity compared to Cr₂AlC, highlighting their potential in biomedical applications.

KEYWORDS

sol-gel, metal carbide, MAX phase, biomedical applications, *Candida albicans*, HepG2

1 Introduction

MAX phases are synthesized by various methods at high temperatures. Different methods also prepared the Cr₂AlC MAX phase. Here, the question is what are the lowest temperature and cost-effective achievable methods for synthesizing MAX Phases? Firstly, the Cr₂GaC MAX phase was synthesized by the sol-gel method at low temperatures (Siebert et al., 2019). Classifications of MAX phases can be delineated



according to distinct ‘n’ values, encompassing M_2AX (211), M_3AX_2 (312), and M_4AX_3 (413) phases, respectively (Sun, 2011). The distinctive combination of weakened M-A bonds and robust M-X bonds, coupled with a nano-layered structure, imparts to these solids a unique amalgamation of metallic properties and biological applications. Other MAX phases include 312 and 413 of Ti_2AlC (Rampai and Tokoloho, 2011; Galvin et al., 2018; Gao et al., 2020; Poulou et al., 2021). The synthesis of the Cr_2AlC MAX phase involves various methods such as the molten salt method (Abdelkader, 2016), ball milling (Ta et al., 2021; Mansouri et al., 2023), chemical vapor deposition (CVD) (Gorshkov et al., 2017), Physical vapor deposition (PVD) (Rueß et al., 2021; Li et al., 2024) and, notably, the sol-gel method. In the previous literature, the sol-gel method was utilized to fabricate the Cr_2GaC MAX phase (Siebert et al., 2019). This research investigated two materials, Cr_2AlC MAX phase, and Cr_2CT_x MXene-Cr, for their potential biomedical applications. Both materials showed free radical scavenging activity, with MXene-Cr being more effective. MXene-Cr also inhibited the enzyme alpha-amylase and displayed strong DNA nuclease activity. Furthermore, both materials exhibited significant antimicrobial activity against various bacteria, with better effects on Gram-positive bacteria. Notably, they inhibited microbial growth at low concentrations and MXene-Cr showed promising antibiofilm activity. Additionally, MXene-Cr demonstrated impressive antibiofilm activity against *S. aureus* (89.86%) and *P. aeruginosa* (87.01%), while the MAX phase displayed an antibiofilm activity exceeding 90%. These findings suggest promising potential for both materials in various biomedical applications (Kaya et al., 2024).

Originating from the mid-1800s, early investigations into silica gels form the foundational basis for the widely employed sol-gel chemistry, a method extensively applied in the synthesis of inorganic solids (Hench and West, 1990). Within the sol-gel methodology, the initial step entails the creation of a colloidal suspension termed “sol,”

which then undergoes a structural transformation into a network referred to as a “gel.”

Various synthesis methods are utilized for Cr_2AlC MAX phase fabrication, including the molten salt method (Liu et al., 2020; Shamsipoor et al., 2021; Liu et al., 2023), ball milling (Mansouri et al., 2023), chemical vapor deposition (CVD) (Lei and Lin, 2022), physical vapor deposition (PVD) (Gonzalez-Julian, 2021), and spark plasma sintering (Duan et al., 2015). Recent research has highlighted the potential of MAX phases as effective high-temperature coatings, with applications spanning turbojets, aircraft, automobiles, and the petrochemical industry. J Liu et al. Successfully produced Cr_2AlC thin films, a type of MAX coating, using magnetron sputtering techniques (Li et al., 2018; Liu et al., 2018). Both elemental and compound targets are employed for the deposition process, with substrate heating or post-annealing necessary to achieve crystallization. However, despite these efforts, challenges persist in achieving the desired stoichiometric ratio and homogeneity due to the presence of binary carbides or intermetallic impurities in the resulting thin films. Manoun et al. synthesized Cr_2AlC compounds by employing a Hot Isostatic Pressing (HIP) method. The synthesis involved mixing Cr, Al, and C, followed by subjecting the mixture to conditions of 1,200°C and approximately 100 MPa pressure (Manoun et al., 2006). Yukhvid et al. employed a self-propagating high-temperature synthesis (SHS) technique to prepare Cr_2AlC . The synthesis involved utilizing mixtures of Cr_2O_3 , CrO_3 , Al, and C, conducted under an argon gas atmosphere at 5 MPa pressure (Gorshkov et al., 2018). Additionally, the reaction kinetics and mechanical properties of the Cr_2AlC compound was investigated, which was synthesized via the hot pressing (HP) technique at 1,300 °C and 30 MPa (Yan et al., 2019). Despite their merits, these methods typically necessitate elevated temperatures (>1,000°C), high pressures (up to 100 MPa), and sophisticated equipment, thereby limiting their widespread

applicability (Lin et al., 2022). Previous studies have predominantly utilized various compounds such as Al_4C_3 , AlCr_2 , Cr_2O_3 , and CrCx (where $x = 0.5$) as raw materials to mitigate the risk of secondary compound formation during processing (Rajkumar et al., 2017). Generally, synthesizing the Cr_2AlC MAX phase directly from a mixture of elemental C, Al, and Cr powders is challenging due to the likely formation of intermediate phases such as Cr_xC_y and Al-C compounds, as well as the oxidation tendency of Al and Cr (Tian et al., 2008). Consequently, there have been limited reports on the fundamental synthesis of the Cr_2AlC MAX phase from elemental powders without the need for high-pressure or complex tools (Yan et al., 2017; TAN et al., 2019).

The above-mentioned methods are more expensive and are high-temperature and high-pressure based. Based on the aforementioned studies, ensuring phase purity is of paramount importance for MAX phase materials. This study aimed to create a facile method for producing the Cr_2AlC MAX phase, utilizing elemental powders as initial ingredients without applying pressure. In the initial stages, the sol-gel method was employed to prepare the Cr_2AlC MAX phase. Additionally, the ternary compounds Cr_3AlC_2 and Cr_4AlC_3 , which exhibit similarities to Cr_2AlC MAX phase, were also synthesized using the sol-gel method by adjusting the concentration ratios of chromium nitrate for the 312 and 413 phases. Sol-gel method is cost cost-effective method and easy to maintain. It is low low-temperature-based technique for synthesizing the Cr_2AlC MAX phase. Other phases Cr_3AlC_2 and Cr_4AlC_3 , (312 and 413) are not mentioned in previous studies, but we prepared those phases successfully by using the sol-gel method. The prepared phases are more stable. we called it ternary compounds. Cr_3AlC_2 and Cr_4AlC_3 , are probably MAX phases. Other novel phases of Ti_2AlC are mentioned in the literature (Tzenov and Barsoum, 2000; Sarkar et al., 2024). The MAX phases are synthesized by the novel sol-gel route and applied for the potential biomedical applications. This work's novelty lies in utilizing a cost-effective the sol-gel technique for synthesizing MAX phases with three different ratio. The development of novel MAX phases such as Cr_3AlC_2 and Cr_4AlC_3 was realized using the sol-gel method. The developed materials were successfully confirmed by several analytical techniques with excellent biomedical application. Herein, the facile sol-gel method has been opted for the synthesis of the Cr_2AlC MAX phase and related ternary compounds. In the sol-gel method, nitrate precursors and citric acid are used for the synthesizing of Cr_2AlC , Cr_3AlC_2 , and Cr_4AlC_3 . Comprehensive characterization through X-ray diffraction (XRD), X-ray photoelectron spectroscopy (XPS), scanning electron microscopy (SEM) with energy-dispersive X-ray spectroscopy (EDX), Fourier-transform infrared spectroscopy (FTIR), Raman spectroscopy, confirmed the Cr_2AlC MAX phase and other prepared Cr_3AlC_2 and Cr_4AlC_3 were found to have comparable structural morphology with Cr_2AlC MAX phase with the prepared Cr_2AlC showing promising results across all analyses, and the ternary compounds exhibiting significant characteristics comparable to the Cr_2AlC MAX phase, further validated through a comparative analysis with the 211 MAX phase. The prepared materials were assessed for biomedical applications including Anti-bacterial, Anti-fungal, and Anti cancerous. The anti-bacterial activity was done against *E coli* and *S. aureus*, anti-fungal

activity against *Candida albicans*, and anti-cancerous activity against the HepG2 cell line (liver cancer cell). The thorough characterization and biomedical assessments underscore the potential of these materials for various applications, offering insights into their structural, chemical, and functional properties, and positioning them as valuable candidates for future research and technological advancements. The realm of material science has been perennially enriched by the discovery and synthesis of novel materials that offer a blend of desirable properties for a wide range of applications.

2 Materials

The chemicals used in this study are Chromium (III) Nitrate Nonahydrate [$\text{Cr}(\text{NO}_3)_3 \cdot 9\text{H}_2\text{O}$, 99.9%, Honeywell], Aluminum Nitrate Nonahydrate [$\text{Al}(\text{NO}_3)_3 \cdot 9\text{H}_2\text{O}$, 99.9%, ChemPUR], and Citric Acid [99.5%, Alfa Aesar]. The deionized water was used throughout the research. All the chemicals used were of analytical grade and used without further purification (Siebert et al., 2019).

2.1 Synthesis of Cr_2AlC , Cr_3AlC_2 , and Cr_4AlC_3 MAX phases

In this experimental procedure, For the 2:1 ratio, 16.0 g of $\text{Cr}(\text{NO}_3)_3 \cdot 9\text{H}_2\text{O}$ and 7.5 g of $\text{Al}(\text{NO}_3)_3 \cdot 9\text{H}_2\text{O}$ were used as precursors, along with 8.4 g (9 equivalents) of citric acid. This same amount of $\text{Al}(\text{NO}_3)_3 \cdot 9\text{H}_2\text{O}$ and citric acid was used for the 3:1 and 4:1 ratios, while the amount of $\text{Cr}(\text{NO}_3)_3 \cdot 9\text{H}_2\text{O}$ was increased to 24.0 g and 32.0 g, respectively. The precursor chemicals were dissolved in water using a magnetic stirrer bar in a beaker. The resulting mixture was then heated within a temperature range of 70°C–80°C, forming a viscous liquid. Once it gelled, the material was moved to an Al_2O_3 crucible for subsequent heat treatment. This annealing process occurred in a horizontal tube furnace (Carbolite) at 900°C in a Nitrogen atmosphere (N_2 , 99.99% purity), with 2°C/min heating rate. The temperature was maintained for 5 hours before allowing the sample to cool gradually to room temperature. Various materials were heated at a temperature of 900°C for 5 hours to gain a deeper understanding of the reaction dynamics. Following thermal treatment, the specimens underwent a 30-min grinding process. After this initial grinding, further grinding was carried out before subjecting the samples to comprehensive characterization using various analytical techniques (Siebert et al., 2019). The schematic diagram of synthesis is shown in Figure 1.

2.2 Characterizations

The Cr_2AlC , Cr_3AlC_2 , and Cr_4AlC_3 samples generated in the synthesis were subjected to a series of analytical techniques for comprehensive characterization. A Bruker D2 Phaser X-ray Diffractometer equipped with Cu-K α radiation ($\lambda = 1.5406 \text{ \AA}$). The scanning range extended from 20° to 70° in terms of 2 θ . Particle size and morphology were examined through SEM Cube II, Emcraft South Korea with EDX. Vibrational spectra were

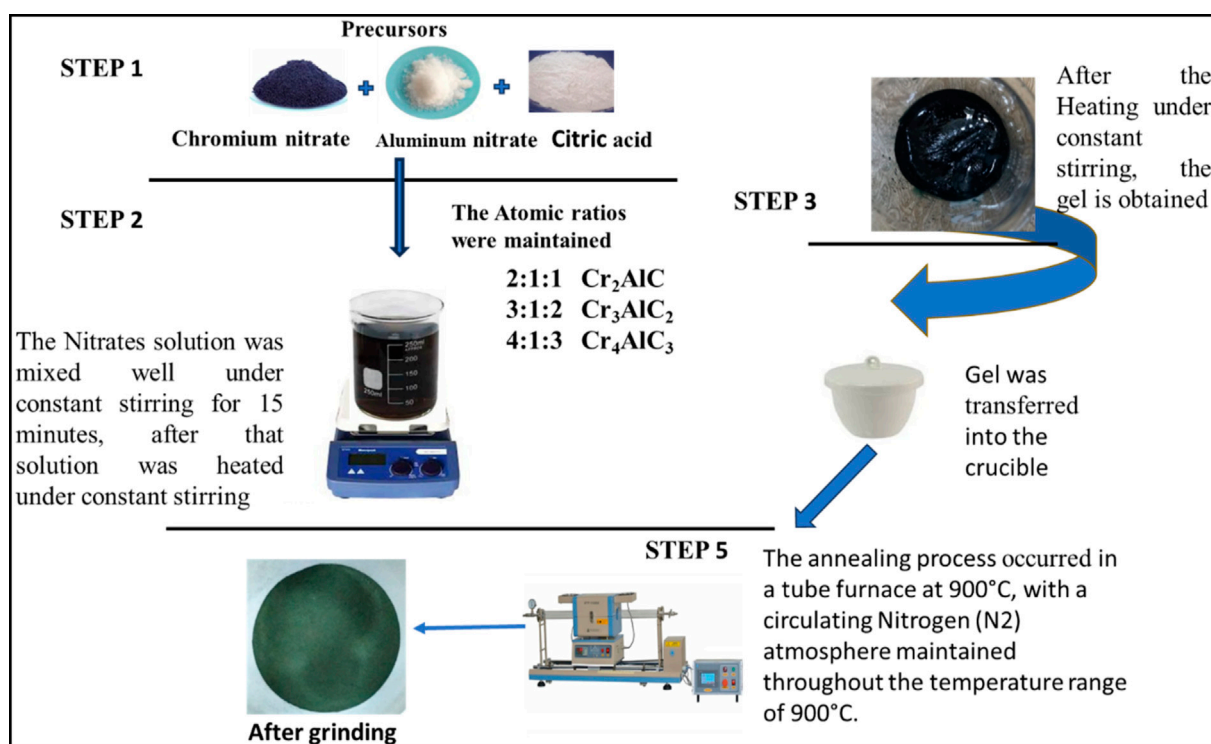


FIGURE 1 Schematic Diagram for the synthesis of Chromium Aluminum Carbide MAX Phases ($\text{Cr}_x\text{AlC}_{x-1}$).

obtained using the Confocal Micro Raman MNSTEX PRI 100, DONGWOO South Korea system. The diverse stretching and bending vibrations of functional groups within the synthesized materials were identified using Fourier Transform Infrared Spectroscopy (FTIR) with an Agilent Technology Cary 360 FTIR spectrophotometer. Additionally, X-ray Photoelectron Spectroscopy (XPS) analysis, performed with ESCALAB-250 (Thermo Scientific, United Kingdom), delved into the electronic states present in the material. 1mL Dimethyl sulfoxide (DMSO) was used to prepare the 40 mg/mL dose to perform biomedical activity. Strains of *E. Coli*, *B. cereus*, and strains of Fungi were assembled from the Department of Microbiology lab in Govt. College University Faisalabad, Pakistan.

2.3 Antifungal activity

The procedure involves creating *Candida albicans* inoculum in Sabouraud Dextrose Broth, adjusting turbidity, and applying MAX Phase materials to agar plates (Bakht et al., 2011). Plates were incubated, and inhibition zones around the MAX Phase material were measured to assess antifungal effectiveness.

2.4 Anti-bacterial activity

This involves preparing *E. coli* inoculum in LB broth, followed by turbidity adjustment, and applying MAX Phase materials on agar plates. Followed by incubation, zones of inhibition are observed to

assess antibacterial effectiveness the same procedure applied for Cr_3AlC_2 and Cr_4AlC_3 .

2.5 Anti-bacterial activity against *S. aureus*

A standardized procedure was opted by preparing *S. aureus* inoculum, applying MAX Phase materials on Mueller-Hinton agar plates, and observing inhibition zones after incubation to assess antibacterial effectiveness (Sharmin et al., 2021). The same method was applied for Cr_3AlC_2 and Cr_4AlC_3 .

2.6 Anti-cancerous activity

Protocol for assessing cytotoxicity on HepG2 ([HEPG2]-HB-8065-ATCC) cells includes culturing cells, treating with Cr_2AlC MAX phase materials, performing MTT assay, and analyzing data to determine IC50 value (Younas et al., 2021). The systematic approach ensures accurate evaluation of cytotoxic effects.

3 Results and discussion

3.1 Material's characterization

The analysis using Fourier transform infrared (FTIR) spectroscopy was performed to ascertain the chemical properties of the synthesized material. FTIR analysis was accomplished to illustrate the surface

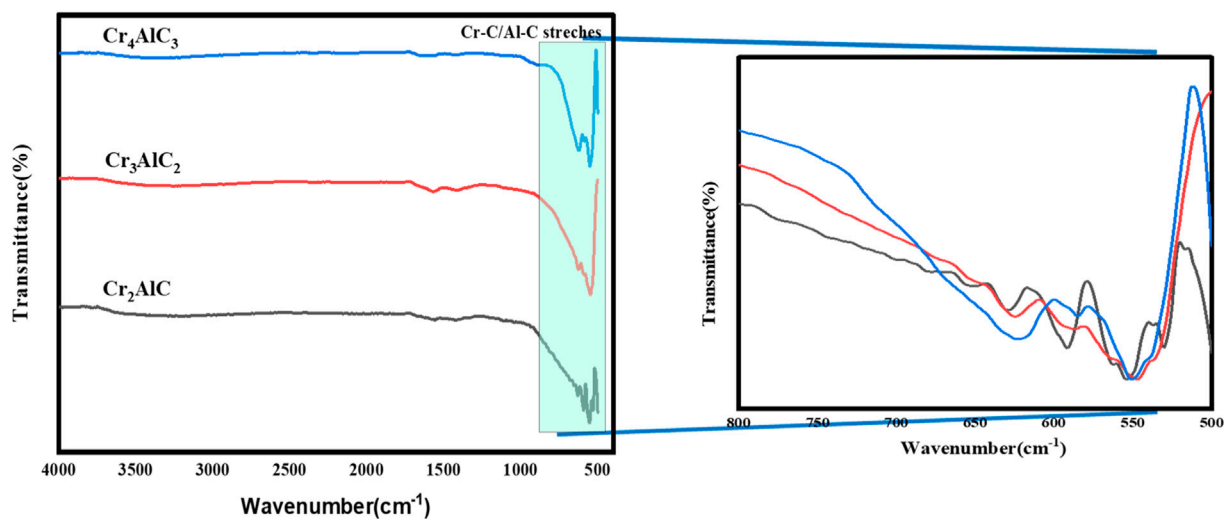


FIGURE 2
FTIR Analysis of prepared samples of Cr_2AlC , Cr_3AlC_2 , and Cr_4AlC_3 .

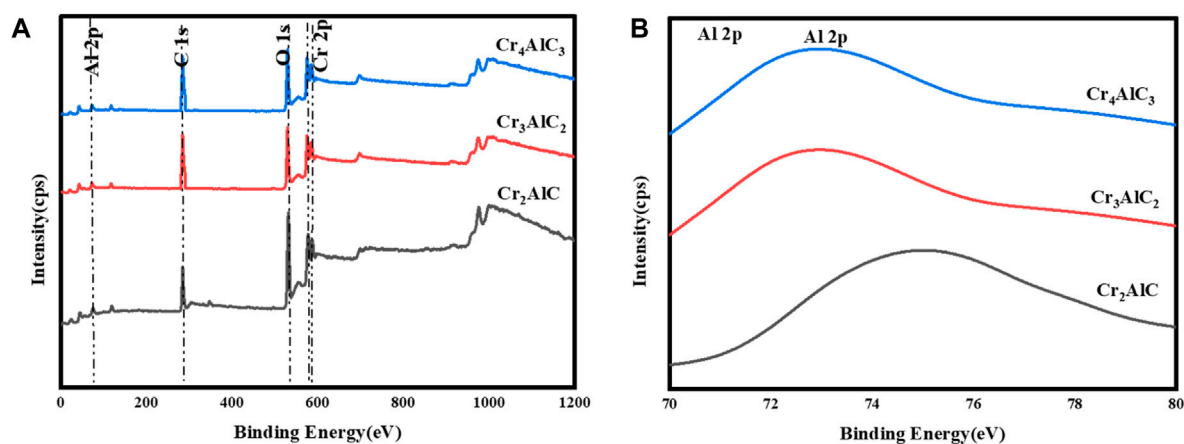


FIGURE 3
(A) XPS analysis of prepared Cr_2AlC , Cr_3AlC_2 , and Cr_4AlC_3 . (B) High resolution XPS spectra of Al 2p.

functional groups present in the Cr_2AlC , Cr_3AlC_2 , and Cr_4AlC_3 (Figure 2). The peaks observed between 430 and 820 cm^{-1} corresponded to the stretching vibration modes of Al-O and Cr-O bonds, indicating the presence of Cr-C and Al-C bonds (Reghunath et al., 2021) for Cr_2AlC , Cr_3AlC_2 , and Cr_4AlC_3 . The FTIR characteristics of prepared Cr_3AlC_2 and Cr_4AlC_3 were aligned with the FTIR spectrum of the Cr_2AlC MAX phase. Peaks appeared between 550 and 800 cm^{-1} are ascribed to the Al-C bonding. In all the FTIR spectra the presence of peaks can be realized confirming the Al-C stretching vibration mode (Shalini Reghunath et al., 2021).

To investigate the surface composition and valence states of the Cr_2AlC MAX phase, XPS analysis of its structural elements was conducted. The results are illustrated in Figure 3. The survey scan of the Cr_2AlC Max phase, Cr_3AlC_2 , and Cr_4AlC_3 are presented in Figure 3A. The presence of Cr, Al, O, and C elements was confirmed, aligning with findings from prior research (Wei et al.,

2015; Soundiraraju et al., 2020). In the high-resolution spectra of the Cr_2AlC Max phase, the Cr spectrum (Figure 4A) exhibits discernible peaks at 575.0 eV and 586.4 eV for Cr 2p (i.e., 2p_{3/2} and 2p_{1/2} respectively). These peaks are indicative of the presence of the Cr-C bond characteristic of chromium carbide, consistent with findings reported by Zamulaeva and co-workers (Zamulaeva et al., 2016). Peaks corresponding to Al 2p were detected at 73.9 eV (Figure 3B) (Hauert et al., 1993), attributed to the Al-C bond. The strong reactivity between aluminum and carbon facilitates the formation of a layered Cr_2AlC structure, characterized by alternating layers of chromium and aluminum. In the C1s spectrum (Figure 4B), a peak at 282.4 eV is attributed to the Cr-C bond (Zamulaeva et al., 2013). Therefore, the high-resolution XPS results suggest the formation of a high-purity Cr_2AlC MAX phase (Monireh et al., 2023a). In Cr_3AlC_2 , the Cr spectrum (Figure 4C) exhibits discernible peaks at 574.8 eV and 584.6 eV for Cr 2p (i.e., 2p_{3/2} and 2p_{1/2} respectively). These peaks are

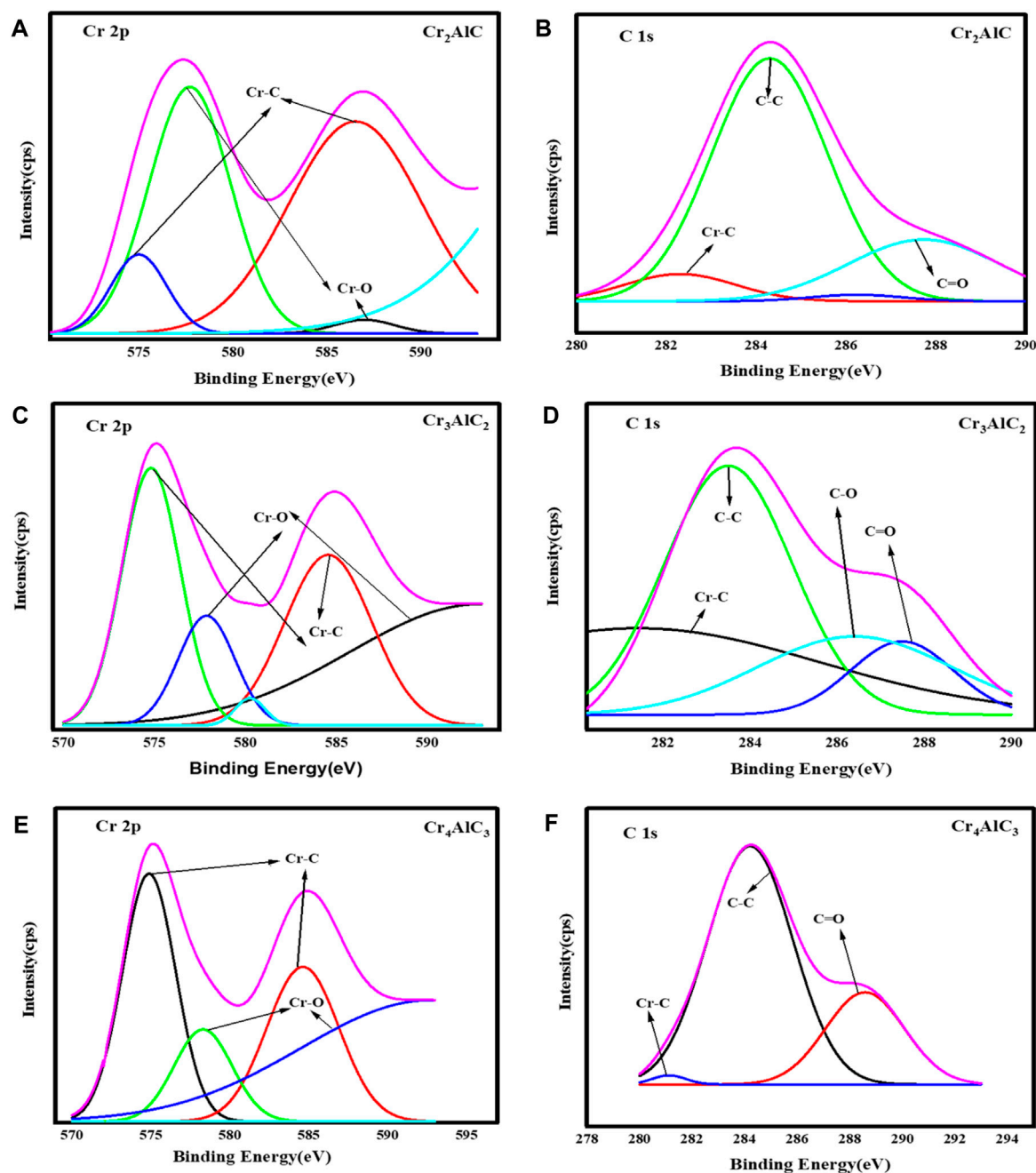


FIGURE 4 High resolution XPS spectra of (A, B) Cr 2p/C 1s for Cr_2AlC , (C,D) Cr 2p/C 1s for Cr_3AlC_2 , and (E,F) Cr 2p/C 1s for Cr_4AlC_3 .

indicative of the presence of the Cr-C bond characteristic of chromium carbide. Peaks corresponding to Al 2p were detected at 73.1 eV (Figure 3B), attributed to the Al-C bond. In the C1s spectrum (Figure 4D), a peak at 282.6 eV is attributed to the Cr-C bond. In Cr_4AlC_3 , the Cr spectrum (Figure 4E) exhibits discernible peaks at 574.8 eV and 584.6 eV for Cr 2p (i.e., 2p_{3/2} and 2p_{1/2} respectively). These peaks are indicative of the presence of the Cr-C bond characteristic of chromium carbide. Peaks corresponding to Al 2p were detected at 73.0 eV (Figure 3B), attributed to the Al-C bond. In the C1s spectrum (Figure 4F), a peak at 281.1 eV is attributed to the Cr-C bond. All the results of XPS for Cr_3AlC_2 and Cr_4AlC_3 aligned with

the Cr_2AlC MAX phase. There are some shifts in peaks, which may be due to material and may be due to changes in composition.

The morphologies of prepared Cr_2AlC , Cr_3AlC_2 , and Cr_4AlC_3 were examined by Scanning electron microscope (SEM). The lamellar sheet structure, characteristic of the prepared materials is evident in Figures 5A, C, E. The layers exhibit delamination, with noticeable kink bands present. The uneven structural morphology with varying surface energies reflects versatility in structural composition thereby effective physicochemical characteristics of the materials. All the results of Cr_3AlC_2 and Cr_4AlC_3 agreed with Cr_2AlC . The lamellar sheets were nonuniform in thickness (Sharma and Pandey, 2019; Sharma et al., 2023).

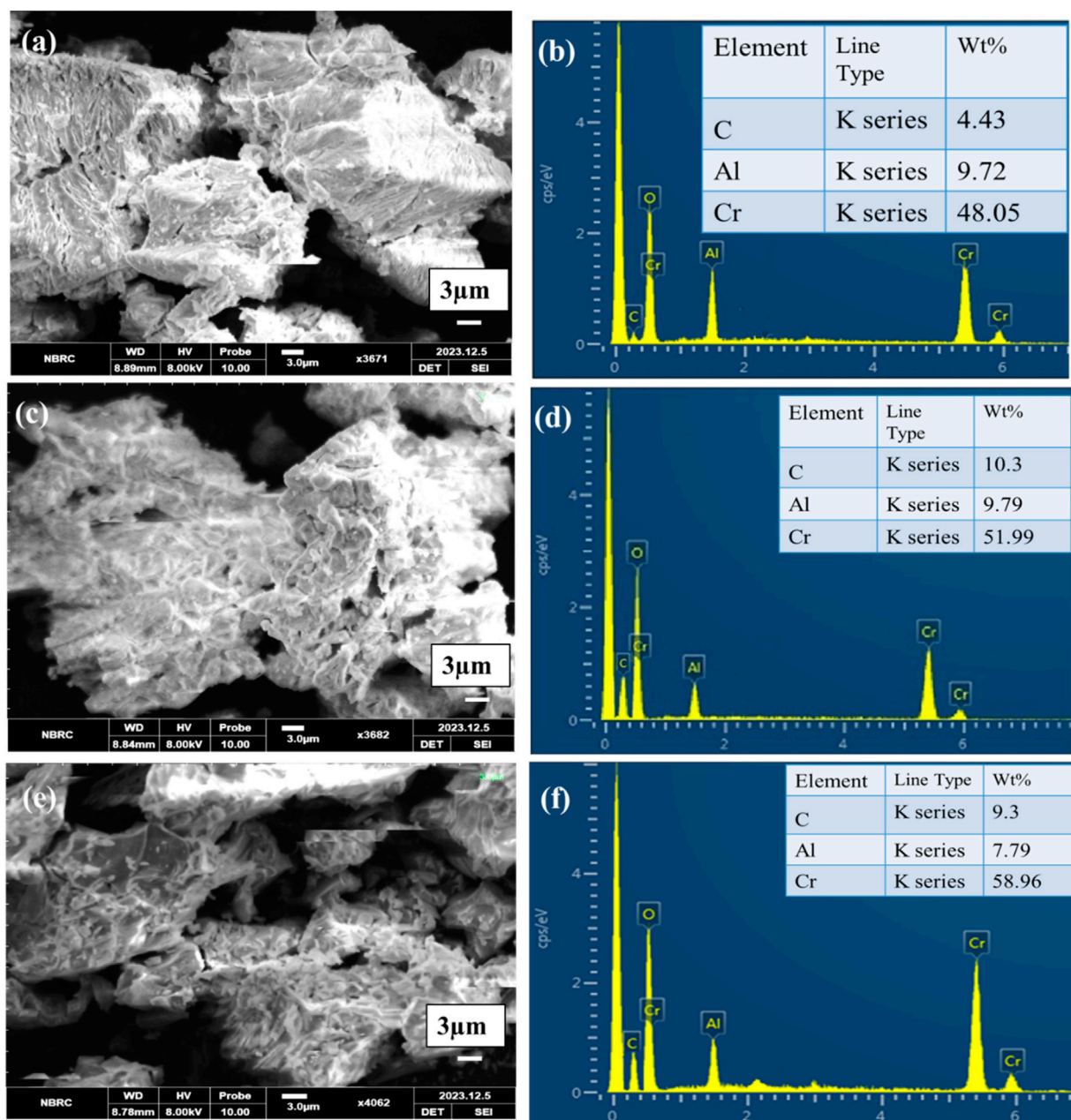


FIGURE 5 SEM-EDX analysis (A,B) Cr₂AlC, (C,D) Cr₃AlC₂, and (E,F) Cr₄AlC₃.

The elemental analysis of the Cr₂AlC, Cr₃AlC₂, and Cr₄AlC₃ powder (Figures 5B, D, F) verified the presence of carbon (C), chromium (Cr), aluminum (Al), and oxygen (O), with no detection of additional elements. Atomic percentages within the EDX spectrum are reported, and the observed values closely correspond to the formula of Cr₂AlC, Cr₃AlC₂, and Cr₄AlC₃ (Monireh et al., 2023b). The expected stoichiometric ratios for Cr₂AlC, Cr₃AlC₂, and Cr₄AlC₃ are 2.5:1:1.0, 2.8:1:2.3 and 3.9:1:2.7 for Cr:Al: C respectively. The obtained ratios closely match this, with a slight excess of Chromium (Cr). These ratios indicate a composition of approximately Cr_{2.5}Al₁C_{1.0}, Cr_{2.8}Al₁C_{2.3}, and Cr_{3.9}Al₁C_{2.7} suggesting a nearly stoichiometric Cr₂AlC, Cr₃AlC₂, and Cr₄AlC₃ with a slight deviation. This deviation could be due to experimental error, sample inhomogeneity, or actual variations in

stoichiometry. The purity of the prepared material in EDX is evident as it only contains Cr, Al, C, and O. There are no other elements present.

The XRD pattern of the Cr₂AlC MAX phase as prepared is displayed in Figure 6A. The distinct sharp peaks observed confirm the formation of the Cr₂AlC MAX phase. Furthermore, the discernible peaks observed at the $2\theta = 22.0^\circ, 24.7^\circ, 26.5^\circ, 36.6^\circ, 42.1^\circ, 50.9^\circ, 55.6^\circ$ and 65.9° correspond to the (0 0 2), (2 1 0), (0 0 4), (1 0 0), (1 0 3), (1 0 4), (1 1 6) and (1 1 0) planes of the synthesized sample, respectively. This observation affirms the hexagonal structure of the prepared MAX phase (Crisan and Crisan, 2018; TUNES et al., 2021). For Cr₃AlC₂ and Cr₄AlC₃ (Figures 6B, C, respectively) all the 2θ values corresponding to the planes were matched with the Cr₂AlC MAX phase. This finding validates the hexagonal structure of the prepared Cr₃AlC₂ and Cr₄AlC₃. Furthermore, the

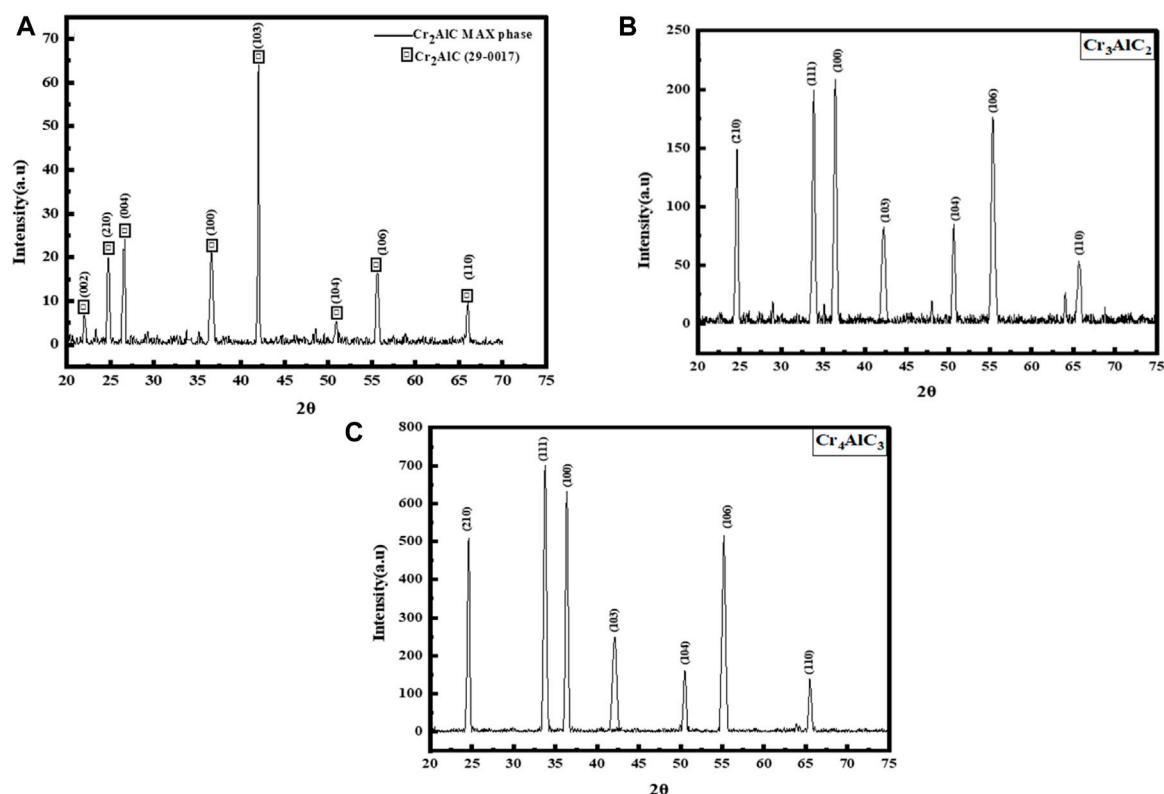


FIGURE 6 XRD analysis of prepared samples of (A) Cr_2AlC , (B) Cr_3AlC_2 , and (C) Cr_4AlC_3 .

crystallite size of the Cr_2AlC was determined to be 55.4 nm using the Debye–Scherrer equation (Zhang et al., 2019) based on the intense XRD peak observed at $2\theta = 42.1^\circ$ (Guan, 2016). Furthermore, the Crystallite size of the Cr_3AlC_2 and Cr_4AlC_3 were determined to be 23.1 nm and 21.3 nm using the Debye–Scherrer equation, based on the intense XRD peak observed at $2\theta = 33.70^\circ$ and 33.50° respectively and the Crystallite size Cr_3AlC_2 and Cr_4AlC_3 were also determined to be 21.8 nm and 23.6 nm using the Debye–Scherrer equation, based on the intense XRD peak observed at $2\theta = 36.4^\circ$ and 36.39° respectively. The values of the lattice constant (a and c) for the hexagonal pattern were designed employing Eq. 1. The equation represents the inter-planar spacing (dhkl) for the plane (hkl) and is expressed as:

$$\frac{1}{d^2} = \left(\frac{h^2}{a^2} + \frac{hk}{a^2} + \frac{k^2}{a^2} + \frac{l^2}{c^2} \right) \quad (1)$$

The determined unit cell parameters are $a = 3.03 \text{ \AA}$ and $c = 12.3 \text{ \AA}$ for the Cr_2AlC MAX phase (Siebert et al., 2019; Reghunath et al., 2021). The unit cell parameters have been determined as follows: for the Cr_3AlC_2 , $a = 2.46 \text{ \AA}$ and $c = 10.28 \text{ \AA}$, and for the Cr_4AlC_3 plane, $a = 2.47 \text{ \AA}$ and $c = 10.31 \text{ \AA}$. The X-ray diffraction (XRD) analysis confirmed the hexagonal structure of the synthesized material. This is further supported by the match between the observed peaks and the reference pattern in JCPDS card no. 29–0017 (Shalini Reghunath et al., 2021). The a and c parameters for Cr_3AlC_2 , and Cr_4AlC_3 aligned with the Cr_2AlC . Cr_3AlC_2 and Cr_4AlC_3 can be probably called MAX phases.

Raman spectroscopy was performed on the samples across a spectral range from 400 cm^{-1} – 2000 cm^{-1} , as illustrated in Figure 7.

The observed peaks at 327 cm^{-1} and 553.8 cm^{-1} , 361.4 cm^{-1} and 553.3 cm^{-1} correspond to the signature peaks of CAC(Cr_2AlC) and Cr_2O_3 , confirming the formation of Cr_2O_3 due to surface oxidation. The obtained results have been confirmed from several relevant publications (Spanier et al., 2005; Shtansky et al., 2009; Bortolozzo et al., 2010; Presser et al., 2012; Vishnyakov et al., 2014; Bentzel et al., 2016; Zhang et al., 2021). Additionally, the peak observed at 809.0 cm^{-1} , 806.7 cm^{-1} and 872.0 cm^{-1} in the Raman spectra of Cr_2AlC , Cr_3AlC_2 , and Cr_4AlC_3 respectively is attributed to the vibrational mode of the carbide (Bortolozzo et al., 2007). The Raman spectrum showed the D band at a Raman shift of $1,356.1 \text{ cm}^{-1}$, $1,359.2 \text{ cm}^{-1}$ and $1,360.4 \text{ cm}^{-1}$ and the G band at a Raman shift of $1,563.3 \text{ cm}^{-1}$, $1,568.4 \text{ cm}^{-1}$, and $1,565.3 \text{ cm}^{-1}$ for Cr_2AlC , Cr_3AlC_2 , and Cr_4AlC_3 respectively. Carbon's D peaks are observable at $1,356.1 \text{ cm}^{-1}$, $1,359.2 \text{ cm}^{-1}$ and $1,360.4 \text{ cm}^{-1}$ and G peaks at $1,563.3 \text{ cm}^{-1}$, $1,568.4 \text{ cm}^{-1}$, and $1,565.3 \text{ cm}^{-1}$ for Cr_2AlC , Cr_3AlC_2 , and Cr_4AlC_3 respectively. The G band is referred to as the graphitic band. Its presence indicated the presence of carbon atoms. The D band is also recognized as the disorder-induced band, being linked to structural defects or disorders present in the carbon material. The I_D/I_G intensity ratio for Cr_2AlC , Cr_3AlC_2 , and Cr_4AlC_3 0.86 suggests the presence of disorder and graphitization in the carbon structure (Patel et al., 2023).

3.2 Biomedical applications of Cr_2AlC MAX phase, Cr_3AlC_2 , and Cr_4AlC_3

The Cr_2AlC MAX phase and prepared ternary compounds demonstrate a suppressive effect on the growth of microorganisms.

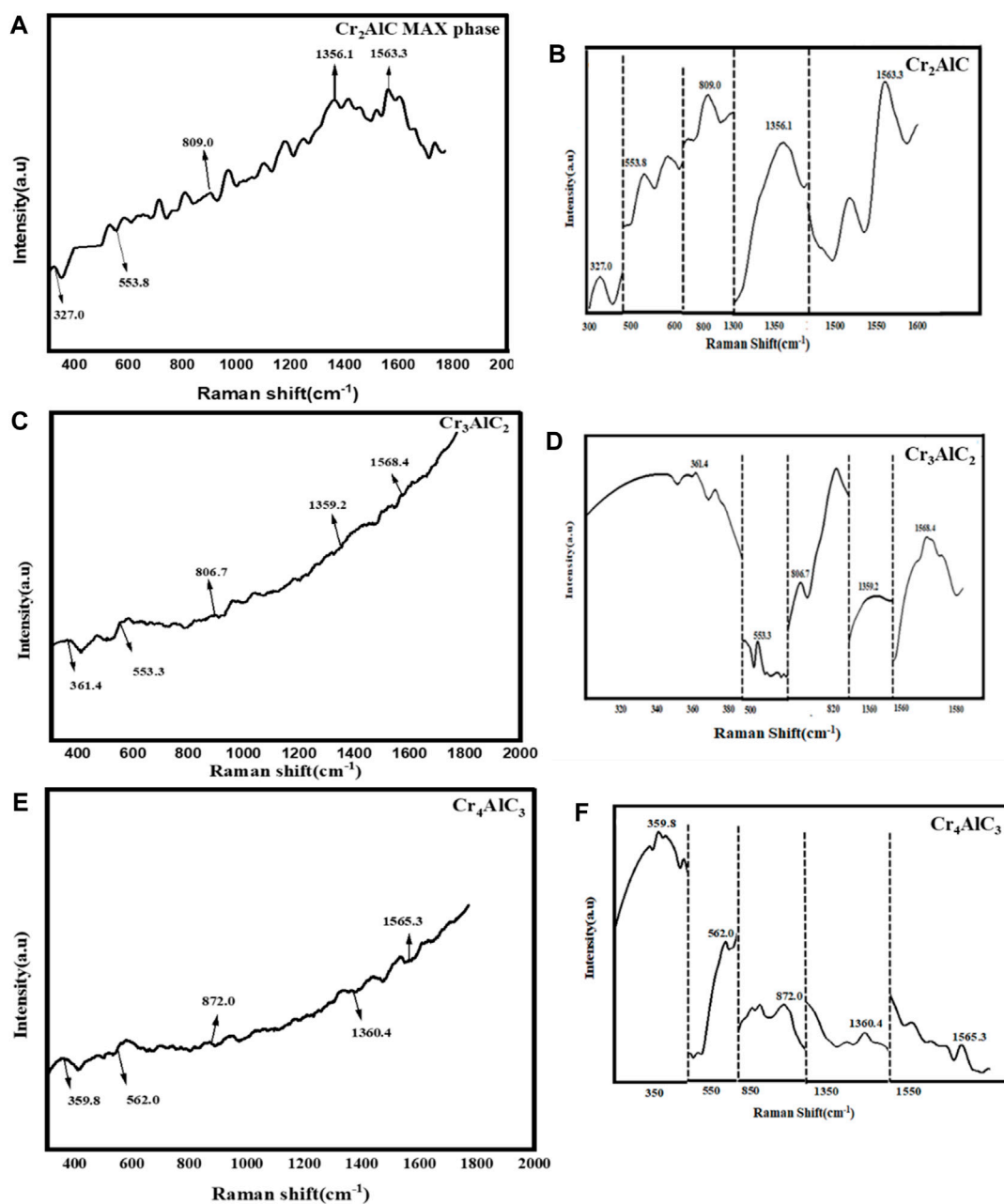


FIGURE 7
Raman spectra for (A,B) Cr_2AlC , (C,D) Cr_3AlC_2 , and (E,F) Cr_4AlC_3 .

It enhances the production of reactive oxygen species (ROS), which in turn disrupts the integrity of cell walls and membrane structures. This disruption impairs vital cellular functions such as DNA and RNA synthesis and increases the susceptibility of microorganisms to ROS. The approach for evaluating biomedical activity (such as antibacterial, antifungal, and anticancer effects) remains consistent and its schematic view is shown in Figure 8.

The antimicrobial activity of the samples synthesized via the sol-gel method was examined. It was found that these particles exhibit potent antimicrobial activity at a concentration of 40 mg/mL. In the context of this research article, we can delve into the biomedical applications of the

synthesized Cr_2AlC , Cr_3AlC_2 , and Cr_4AlC_3 particularly focusing on its differential efficacy against *Candida albicans* and bacteria like *E. coli* and *S. aureus* (Chacko et al., 2024). Emphasize its noteworthy antifungal activity, demonstrated by an inhibition zone of 16 mm, 17 mm, and 15 mm (positive control = 15 mm) against *Candida albicans* for Cr_2AlC , Cr_3AlC_2 , and Cr_4AlC_3 respectively, underscoring its potential as an antifungal agent as shown in Figure 9 and Table 1. In contrast, it discussed its lack of effectiveness against both Gram-negative (*E. coli*) and Gram-positive (*S. aureus*) bacteria, exploring potential reasons for this selective antimicrobial activity. Consider factors such as the distinct interaction mechanisms of the Cr_2AlC ,

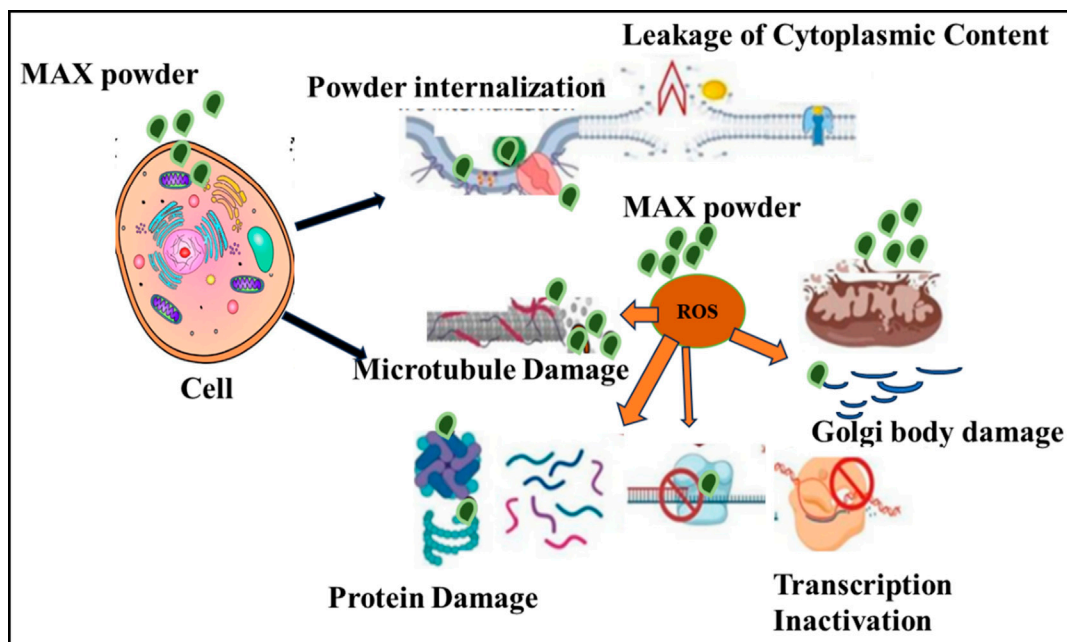


FIGURE 8 Schematic view of biomedical activity mechanism (antibacterial, antifungal, and anticancer) Activity.

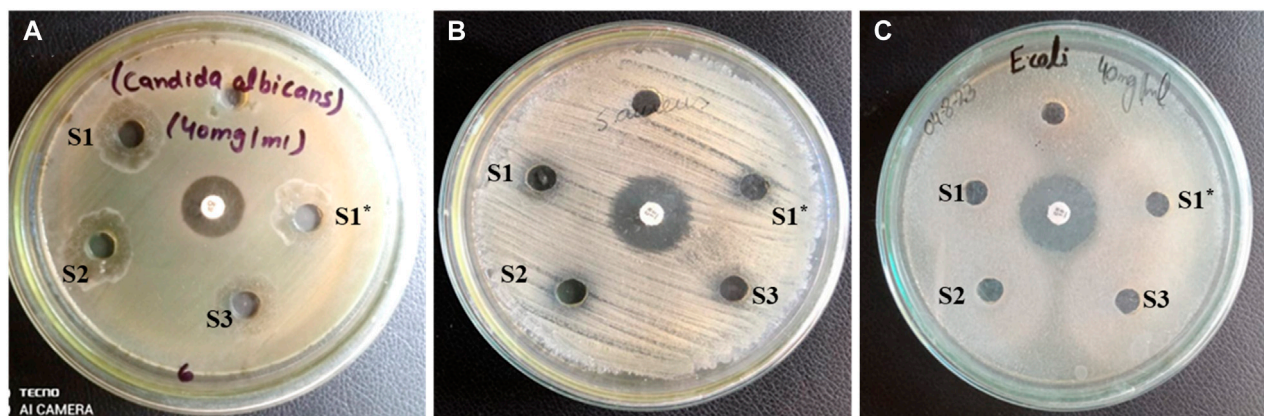
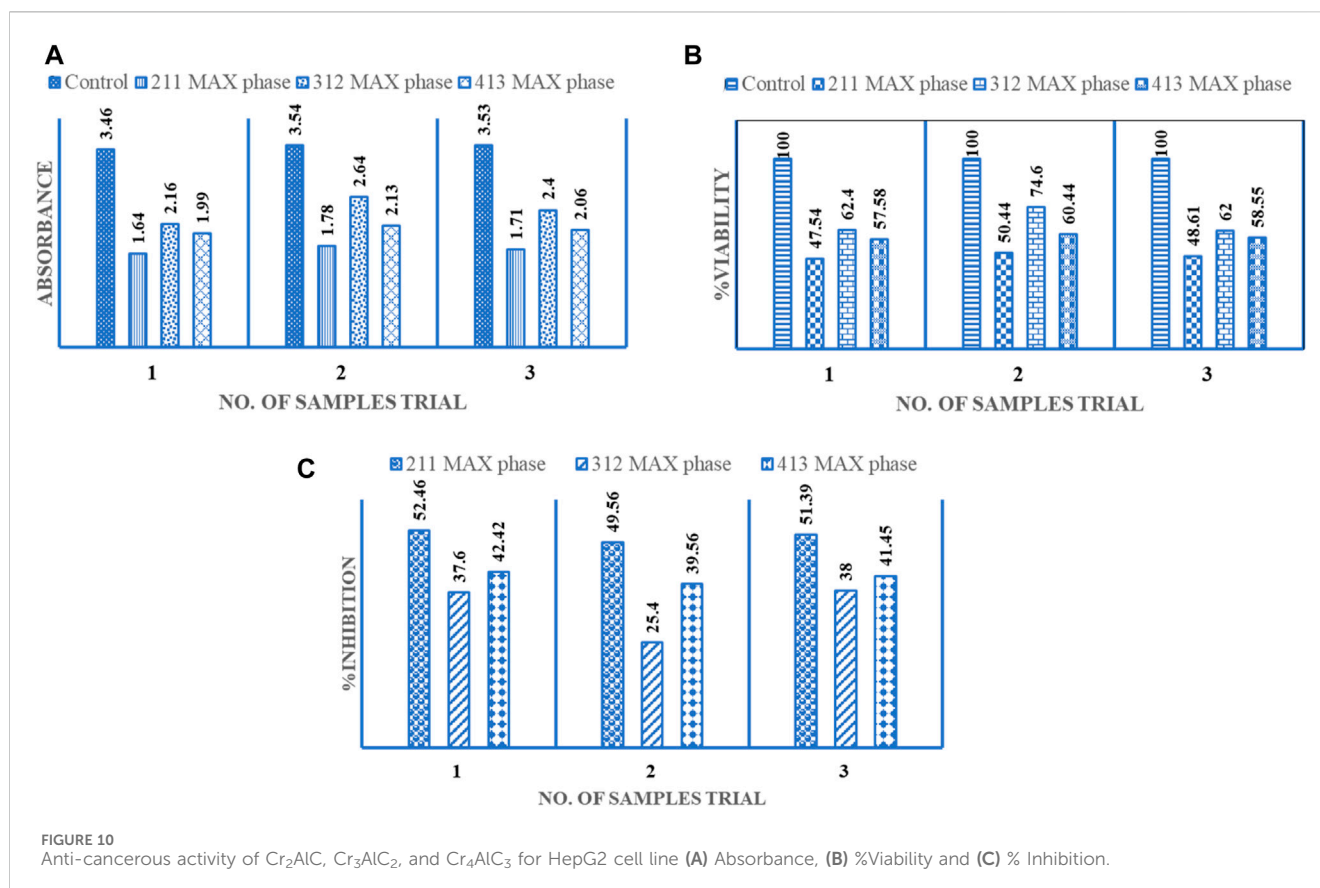


FIGURE 9 (A) Antifungal activity of S1, S1*(Cr₂AlC MAX phase), S2 (Cr₃AlC₂), and S3 (Cr₄AlC₃) for *Candida albicans* (B) for *S. aureus*, and (C) for *E. coli*.

TABLE 1 Antifungal activity of Cr₂AlC, Cr₃AlC₂, and Cr₄AlC₃ for *Candida albicans*.

Sample	<i>Candida albicans</i> dose (40 mg/mL) (Inhibition zones 15 mm)	<i>E. coli</i> Dose (40 mg/mL) (Inhibition zones 23 mm)	<i>S. aureus</i> Dose (40 mg/mL) (Inhibition zones 18 mm)
	Size (mm)	Size (mm)	Size (mm)
S1	16	—	6
S2	17	—	5
S3	15	—	7



Cr_3AlC_2 , and Cr_4AlC_3 with fungal cells versus bacterial cells, or variations in cell wall structures and metabolic pathways between fungi and bacteria (Berardo et al., 2024).

To provide a comprehensive perspective on the biomedical potential of Cr_2AlC , Cr_3AlC_2 , and Cr_4AlC_3 materials, it is imperative to acknowledge their limitations and advocate for further research to enhance understanding and improve antibacterial properties. The antifungal properties of the Cr_2AlC , Cr_3AlC_2 , and Cr_4AlC_3 against *Candida albicans* can be ascribed to various inherent characteristics of nanomaterials like Cr_2AlC , Cr_3AlC_2 , and Cr_4AlC_3 . Nanocomposites possess distinct physical properties, including a large specific surface area and unique interaction mechanisms with fungal cells, enabling effective targeting and inhibition of fungal growth. Conversely, the lack of efficacy against bacteria such as *E. coli* and *S. aureus* may be attributed to disparities in cell wall structures and metabolic pathways between fungi and bacteria (El-Zahed et al., 2024). Bacteria typically exhibit more complex and robust cell wall structures, potentially rendering them less susceptible to the mechanisms employed by Cr_2AlC , Cr_3AlC_2 , and Cr_4AlC_3 nanomaterials. Moreover, the interaction mechanisms of these nanomaterials may be more potent against fungi's cell structures and reproductive mechanisms than bacteria. This specificity in antimicrobial activity underscores the significance of comprehending the intricate interactions between nanomaterials and various microorganisms for the advancement of targeted antimicrobial therapies (Warsi et al., 2022; Krasian et al., 2024).

3.3 Anti-cancerous activity

The established medical use of synthesized Cr_2AlC , Cr_3AlC_2 , and Cr_4AlC_3 extends to treating various types of cancer cells (Khaled et al., 2024). The prepared samples of Cr_2AlC , Cr_3AlC_2 , and Cr_4AlC_3 were evaluated for their anti-cancer activity against liver cancer HepG2 cell line was conducted. The cells underwent treatment with a 200 $\mu\text{g}/\text{mL}$ dosage for 48 h. In this investigation, the cytotoxic impact of Cr_2AlC , Cr_3AlC_2 , and Cr_4AlC_3 was evaluated on HepG-2 (human hepatocellular cancer cells), uncovering pronounced cytotoxicity against the HepG-2 cells. Particularly, at a concentration of 200 $\mu\text{g}/\text{mL}$, that composite exhibited noteworthy anti-cancer activity by markedly inhibiting the growth of hepatocellular carcinoma and reducing cellular viability in HepG-2 cells, as illustrated in Figure 10 (Al-Thubaiti et al., 2022; Kumar et al., 2024). Three distinct plots illustrate data for absorbance, Viability%, and % inhibition in the graphical depiction. The minimum absorbance value was observed as 1.64 (mean value 1.71, S. D 0.05), 2.4 (mean value 2.4, S. D 0.19), and 1.99 (mean 2.06, S. D 0.05) for Cr_2AlC , Cr_3AlC_2 , and Cr_4AlC_3 respectively, as showed in Figure 10A and the maximum viability value was recorded as 50.4% (mean value 48.86, S. D 1.46), 62.4 (mean value 66.3, S. D 5.84) and 60.4 (mean value 58.8, S. D 1.18) as indicated in Figure 10B for Cr_2AlC , Cr_3AlC_2 , and Cr_4AlC_3 respectively. Figure 10C represented the maximum inhibition value observed as 52.46% (mean value 51.13, S. D 1.19), 38 (mean value 33.6, S. D 5.84), and 42.4 (mean value 41.1, S. D 1.18) for Cr_2AlC , Cr_3AlC_2 , and Cr_4AlC_3 respectively (Sedky et al., 2024).

4 Conclusion

In the initial attempt, a cost-effective sol-gel approach was utilized to synthesize Cr_2AlC , Cr_3AlC_2 , and Cr_4AlC_3 MAX phases. This novel synthesis method successfully produced these compounds through a sol-gel wet chemistry approach. Various characterization techniques were employed to confirm the formation of the MAX phases. The synthesized powders exhibited hexagonal structures, indicating high purity and stability. One notable advantage of this wet chemical technique was its enhanced handling of the precursor mixture, resulting in the formation of lamellar sheet structures for Cr_2AlC , Cr_3AlC_2 , and Cr_4AlC_3 . Analysis of X-ray diffraction data confirmed the presence of highly crystalline Cr_2AlC , Cr_3AlC_2 , and Cr_4AlC_3 , along with minor quantities of additional phases such as Cr_2O_3 and Cr_3C_2 . Modifying the precursor mixture by increasing the excess of citric acid showed promise in reducing the level of oxide content in the final products. Furthermore, the synthesized materials exhibited notable antifungal efficacy against *Candida albicans*. Their anti-cancer activity was evaluated against the HepG2 cell line, with minimum absorbance values observed as follows: 1.64 (mean value 1.71, S.D 0.05) for Cr_2AlC , 2.4 (mean value 2.4, S.D 0.19) for Cr_3AlC_2 , and 1.99 (mean value 2.06, S.D 0.05) for Cr_4AlC_3 . Maximum viability values were recorded as 50.4% (mean value 48.86, S.D 1.46) for Cr_2AlC , 62.4% (mean value 66.3, S.D 5.84) for Cr_3AlC_2 , and 60.4% (mean value 58.8, S.D 1.18) for Cr_4AlC_3 . Additionally, maximum inhibition values were observed as 52.46% (mean value 51.13, S.D 1.19) for Cr_2AlC , 38% (mean value 33.6, S.D 5.84) for Cr_3AlC_2 , and 42.4% (mean value 41.1, S.D 1.18) for Cr_4AlC_3 .

Data availability statement

The raw data supporting the conclusion of this article will be available upon request.

Ethics statement

Ethical approval was not required for the studies on animals in accordance with the local legislation and institutional requirements because only commercially available established cell lines were used.

References

- Abdelkader, A. M. (2016). Molten salts electrochemical synthesis of Cr_2AlC . *J. Eur. Ceram. Soc.* 36 (1), 33–42. doi:10.1016/j.jeurceramsoc.2015.09.003
- Al-Thubaiti, E. H., El-Megharbel, S. M., Albogami, B., and Hamza, R. Z. (2022). Synthesis, spectroscopic, chemical characterizations, anticancer capacities against HepG-2, antibacterial and antioxidant activities of cefotaxime metal complexes with Ca (II), Cr (III), Zn (II), Cu (II) and Se (IV). *Antibiotics* 11 (7), 967. doi:10.3390/antibiotics11070967
- Bakht, J., Islam, A., and Shafi, M. (2011). Antimicrobial potential of *Eclipta alba* by well diffusion method. *Pak. J. Bot.* 43, 161–166.
- Bentzel, G. W., Naguib, M., Lane, N. J., Vogel, S. C., Presser, V., Dubois, S., et al. (2016). High-temperature neutron diffraction, Raman spectroscopy, and first-principles calculations of Ti_3SnC_2 and Ti_2SnC . *Raman Spectrosc. first-principles Calc. Ti3SnC2 Ti2SnC J. Am. Ceram. Soc.* 99 (7), 2233–2242. doi:10.1111/jace.14210
- Berardo, M. E. V., Mendieta, J. R., Villamonte, M. D., Colman, S. L., and a, D. N. (2024). Antifungal and antibacterial activities of Cannabis sativa L. resins. *J. Ethnopharmacol.* 318, 116839. doi:10.1016/j.jep.2023.116839
- Bortolozzo, A., Serrano, G., Serquis, A., Rodrigues, D., Jr, Dos Santos, C., Fisk, Z., et al. (2010). Superconductivity at 7.3 K in Ti_2InN . *Solid State Commun.* 150 (29–30), 1364–1366. doi:10.1016/j.ssc.2010.04.036
- Bortolozzo, A. D., Sant'Anna, O. H., Santos, C. A. M. d., and Machado, A. J. S. (2007). Superconductivity in the hexagonal-layered nanolaminates Ti_2InC compound. *Solid State Commun.* 144 (10–11), 419–421. doi:10.1016/j.ssc.2007.09.028
- Chacko, S. K., Balakrishnan, R., Kalarikkal, N., and Thomas, N. G. (2024). Ternary fiber mats of PVDF-HFP/cellulose/LiFe5O8 nanoparticles with enhanced electric, magnetoelectric, and antibacterial properties: a promising approach for magnetic and electric field-responsive antibacterial coatings. *ACS Appl. Polym. Mater.* 6 (2), 1429–1438. doi:10.1021/acsapm.3c02588
- Crisan, O., and Crisan, A. D. (2018). Incipient low-temperature formation of MAX phase in Cr–Al–C films. *J. Adv. Ceram.* 7, 143–151. doi:10.1007/s40145-018-0265-5
- Duan, X., Shen, L., Jia, D., Zhou, Y., Zwaag, S. v. d., and Sloof, W. G. (2015). Synthesis of high-purity, isotropic or textured Cr_2AlC bulk ceramics by spark plasma sintering of pressure-less sintered powders. *J. Eur. Ceram. Soc.* 35 (5), 1393–1400. doi:10.1016/j.jeurceramsoc.2014.11.008

Author contributions

MS: Data curation, Formal Analysis, Methodology, Writing–original draft. NS: Conceptualization, Resources, Supervision, Writing–review and editing. NA: Software, Validation, Writing–review and editing. ZZ: Investigation, Validation, Writing–original draft. MZ: Methodology, Resources, Visualization, Writing–review and editing.

Funding

The author(s) declare that no financial support was received for the research, authorship, and/or publication of this article.

Acknowledgments

The authors extend thanks to Dr. Imran Shahid, Qatar University for characterization and to Dr. Azhar Rasul, Department of Zoology, GC University Faisalabad, Pakistan for biological and anticancer activities. This cell line was gifted by Prof. Dr. Xiaomeng Li, Northeast Normal University, China to Dr. Azhar Rasul, Department of Zoology, GC University Faisalabad, Pakistan.

Conflict of interest

The authors declare that the research was conducted in the absence of any commercial or financial relationships that could be construed as a potential conflict of interest.

Publisher's note

All claims expressed in this article are solely those of the authors and do not necessarily represent those of their affiliated organizations, or those of the publisher, the editors and the reviewers. Any product that may be evaluated in this article, or claim that may be made by its manufacturer, is not guaranteed or endorsed by the publisher.

- El-Zahed, M. M., Diab, M. A., El-Sonbati, A. Z., Saad, M. H., Eldesoky, A. M., and El-Bindary, M. A. (2024). Synthesis, spectroscopic characterization studies of chelating complexes and their applications as antimicrobial agents, DNA binding, molecular docking, and electrochemical studies. *Appl. Organomet. Chem.* 38 (1), e7290. doi:10.1002/aoc.7290
- Galvin, T., Hyatt, N. C., Rainforth, W. M., Reaney, I. M., and Shepherd, D. (2018). Molten salt synthesis of MAX phases in the Ti-Al-C system. *J. Eur. Ceram. Soc.* 38 (14), 4585–4589. doi:10.1016/j.jeurceramsoc.2018.06.034
- Gao, L., Han, T., Guo, Z., Zhang, X., Pan, D., Zhou, S., et al. (2020). Preparation and performance of MAX phase Ti_3AlC_2 by *in-situ* reaction of Ti-Al-C system. *Adv. Powder Technol.* 31 (8), 3533–3539. doi:10.1016/j.apt.2020.06.042
- Gonzalez-Julian, J. (2021). Processing of MAX phases: from synthesis to applications. *J. Am. Ceram. Soc.* 104 (2), 659–690. doi:10.1111/jace.17544
- Gorshkov, V. A., Miloserdov, P. A., Luginina, M. A., Sachkova, N. V., and Belikova, A. F. (2017). High-temperature synthesis of a cast material with a maximum content of the MAX phase Cr_2AlC . *Inorg. Mater.* 53, 271–277. doi:10.1134/s0020168517030062
- Gorshkov, V. A., Miloserdov, P. A., Sachkova, N. V., Luginina, M. A., and Yukhvid, V. I. (2018). SHS metallurgy of Cr_2AlC MAX phase-based cast materials. *Russ. J. Non-Ferrous Metals* 59, 570–575. doi:10.3103/s106782121805005x
- Guan, C. (2016). Synthesis of fine and high purity Cr_2AlC powders by novel method. *Adv. Appl. Ceram.* 115 (8), 505–508. doi:10.1179/1743676115y.0000000026
- Hauert, R., Patscheider, J., Tobler, M., and Zehringer, R. (1993). XPS investigation of the aC: H/Al interface. *Surf. Sci.* 292 (1–2), A605–A129. doi:10.1016/0167-2584(93)90851-9
- Hench, L. L., and West, J. K. (1990). The sol-gel process. *Chem. Rev.* 90 (1), 33–72. doi:10.1021/cr00099a003
- Kaya, G., Koc, E. O., Özdemir, S., Yalçın, M. S., Ocakoglu, K., and Dizge, N. (2024). The syntheses of chromium aluminum carbide (Cr_2AlC) MAX phase and Cr_2CT_x MXene and investigation of their antimicrobial properties. *Appl. Biochem. Biotechnol.* 1–15. doi:10.1007/s12010-024-04910-w
- Khaled, A. M., Othman, M. S., Obeidat, S. T., Aleid, G. M., Aboelnaga, S. M., Fehaid, A., et al. (2024). Green-synthesized silver and selenium nanoparticles using berberine: a comparative assessment of *in vitro* anticancer potential on human hepatocellular carcinoma cell line (HepG2). *Cells* 13 (3), 287. doi:10.3390/cells13030287
- Krasian, T., Punyodom, W., Molloy, R., Topham, P. D., Tighe, B. J., Mahomed, A., et al. (2024). Low cytotoxicity, antibacterial property, and curcumin delivery performance of toughness-enhanced electrospun composite membranes based on poly (lactic acid) and MAX phase (Ti_3AlC_2). *International Journal of Biological Macromolecules*, 129967. *Int. J. Biol. Macromol.* 262, 129967. doi:10.1016/j.ijbiomac.2024.129967
- Kumar, D., Pal, R. R., Das, N., Roy, P., Saraf, S. A., Bayram, S., et al. (2024). Synthesis of flaxseed gum/melanin-based scaffold: a novel approach for nano-encapsulation of doxorubicin with enhanced anticancer activity. *Int. J. Biol. Macromol.* 256, 127964. doi:10.1016/j.ijbiomac.2023.127964
- Lei, X., and Lin, N. (2022). Structure and synthesis of MAX phase materials: a brief review. *Crit. Rev. Solid State Mater. Sci.* 47 (5), 736–771. doi:10.1080/10408436.2021.1966384
- Li, Y., Zhao, G., Qian, Y., Xu, J., and Li, M. (2018). Deposition of phase-pure Cr_2AlC coating by DC magnetron sputtering and post annealing using Cr-Al-C targets with controlled elemental composition but different phase compositions. *J. Mater. Sci. Technol.* 34 (3), 466–471. doi:10.1016/j.jmst.2017.01.029
- Li, Z., Wang, Z., Ma, G., Chen, R., Yang, W., Wang, K., et al. (2024). High-performance Cr_2AlC MAX phase coatings for ATF application: interface design and oxidation mechanism. *Corros. Commun.* 13, 27–36. doi:10.1016/j.corcom.2023.10.001
- Lin, Z., Zhou, Y., Li, M., and Wang, J. (2022). *In-situ* hot pressing/solid-liquid reaction synthesis of bulk Cr_2AlC . *Int. J. Mater. Res.* 96 (3), 291–296. doi:10.3139/146.101033
- Liu, J., Zuo, X., Wang, Z., Wang, L., Wu, X., Ke, P., et al. (2018). Fabrication and mechanical properties of high purity of Cr_2AlC coatings by adjustable Al contents. *J. Alloys Compd.* 753, 11–17. doi:10.1016/j.jallcom.2018.04.100
- Liu, P., Hu, M., Hu, L., Yin, M., Wu, H., and Hu, M. (2020). Fabrication of Cr_2AlC powder by molten salt electrolysis at 850° C with good oxidation resistance. *J. Alloys Compd.* 826, 154003. doi:10.1016/j.jallcom.2020.154003
- Liu, Z., Xu, J., Xi, X., Luo, W., and Zhou, J. (2023). Molten salt dynamic sealing synthesis of MAX phases (Ti_3AlC_2 , Ti_3SiC_2 , et al.) powder in air. *Ceram. Int.* 49 (1), 168–178. doi:10.1016/j.ceramint.2022.08.325
- Manoun, B., Gulve, R. P., Saxena, S. K., Gupta, S., Barsoum, M. W., and Zha, C. S. (2006). Compression behavior of M_2AlC (M= Ti, V, Cr, Nb, and Ta) phases to above 50 GPa. *Phys. Rev. B* 73 (2), 024110. doi:10.1103/physrevb.73.024110
- Mansouri, B., Rafiei, M., Ebrahimzadeh, L., Naeimi, F., and Berekat, M. (2023). The effect of milling time and heat treatment on the synthesis of the Cr_2AlC MAX phase. *Can. Metall. Q.*, 1–11. doi:10.1080/00084433.2023.2251210
- Monireh, A., Alireza, K., Samira, A.-O., Behrouz, V., Yasin, O., and Yejoon, Y. (2023a). Catalytic activation of hydrogen peroxide by Cr_2AlC MAX phase under ultrasound waves for a treatment of water contaminated with organic pollutants. *Ultrason. Sonochemistry* 93, 106294. doi:10.1016/j.ultsonch.2023.106294
- Monireh, A., Alireza, K., Samira, A.-O., Behrouz, V., Yasin, O., and Yejoon, Y. (2023b). Catalytic activation of hydrogen peroxide by Cr_2AlC MAX phase under ultrasound waves for a treatment of water contaminated with organic pollutants. *Ultrason. Sonochemistry* 93, 106294. doi:10.1016/j.ultsonch.2023.106294
- Patel, P. C., Mishra, P. K., and Kandpal, H. C. (2023). Study of MAX phase based Schottky interfacial structure: the case of electron-beam deposited epitaxial Cr_2AlC film on p-Si (100). *J. Mater. Sci.* 58 (9), 4041–4053. doi:10.1007/s10853-023-08286-w
- Poulou, A., Mellan, T. A., and Finnis, M. W. (2021). Stability of Zr-Al-C and Ti-Al-C MAX phases: a theoretical study. *A Theor. study. Phys. Rev. Mater.* 5 (3), 033608. doi:10.1103/physrevmaterials.5.033608
- Presser, V., Naguib, M., Chaput, L., Togo, A., Hug, G., and Barsoum, M. W. (2012). First-order Raman scattering of the MAX phases: Ti_2AlN , $Ti_2AlC_{0.5}N_{0.5}$, Ti_2AlC , $(Ti_{0.5}V_{0.5})_2AlC$, V_2AlC , Ti_3AlC_2 , and Ti_3GeC_2 43(1), 168–172. *J. Raman Spectrosc.* 43 (1), 168–172. doi:10.1002/jrs.3036
- Rajkumar, Y., Rahul, B. M., Akash, P. A., and Panigrahi, B. B. (2017). Nonisothermal sintering of Cr_2AlC powder. *Int. J. Appl. Ceram. Technol.* 14 (1), 63–67. doi:10.1111/ijac.12617
- Rampai, H., and Tokoloho, L. (2011). *Synthesis of Ti_2AlC , Ti_3AlC_2 and Ti_3SiC_2 MAX phase ceramics; and their composites with c-BN.*
- Reghunath, B. S., Davis, D., and Devi, K. R. S. (2021). Synthesis and characterization of Cr_2AlC MAX phase for photocatalytic applications. *Chemosphere* 283, 131281. doi:10.1016/j.chemosphere.2021.131281
- Rueß, H., Werner, J., Unutulmazsoy, Y., Gerlach, J. W., Chen, X., Stelzer, B., et al. (2021). Effect of target peak power density on the phase formation, microstructure evolution, and mechanical properties of Cr_2AlC MAX-phase coatings. *J. Eur. Ceram. Soc.* 41 (3), 1841–1847. doi:10.1016/j.jeurceramsoc.2020.10.072
- Sarkar, S., Banerjee, P., and Raychaudhury, M. D. (2024). *The Elusive member of the Ti-Al-C MAX family- Ti_4AlC_3 .* arXiv preprint arXiv:2402.10621.
- Sedky, N. K., Fawzy, I. M., Hassan, A., Mahdy, N. K., Attia, R. T., Shamma, S. N., et al. (2024). Innovative microwave-assisted biosynthesis of copper oxide nanoparticles loaded with platinum (ii) based complex for halting colon cancer: cellular, molecular, and computational investigations. *RSC Adv.* 14 (6), 4005–4024. doi:10.1039/d3ra08779d
- Shalini Reghunath, B., Davis, D., and Sunaja Devi, K. R. (2021). Synthesis and characterization of Cr_2AlC MAX phase for photocatalytic applications. *Chemosphere* 283, 131281. doi:10.1016/j.chemosphere.2021.131281
- Shamsipour, A., Farvizi, M., Razavi, M., Keyvani, A., Mousavi, B., and Pan, W. (2021). Hot corrosion behavior of Cr_2AlC MAX phase and CoNiCrAlY compounds at 950° C in presence of $Na_2SO_4 + V_2O_5$ molten salts. *Ceram. Int.* 47 (2), 2347–2357. doi:10.1016/j.ceramint.2020.09.077
- Sharma, P., Kainth, S., Singh, K., Mahajan, R. L., and Pandey, O. P. (2023). Investigating non-isothermal oxidation kinetics of a non-stoichiometrically synthesized Ti_3AlC_2 MAX phase. *J. Alloys Compd.* 959, 170488. doi:10.1016/j.jallcom.2023.170488
- Sharma, P., and Pandey, O. P. (2019). Non-isothermal oxidation kinetics of nano-laminated Cr_2AlC MAX phase. *J. Alloys Compd.* 773, 872–882. doi:10.1016/j.jallcom.2018.09.326
- Sharmin, S., Rahaman, M. M., Sarkar, C., Atolani, O., Islam, M. T., and Adeyemi, O. S. (2021). Nanoparticles as antimicrobial and antiviral agents: a literature-based perspective study. *Heliyon* 7 (3), e06456. doi:10.1016/j.heliyon.2021.e06456
- Shtansky, D. V., Kiryukhantsev-Korneev, P. V., Shevko, A. N., Mavrin, B. N., Rojas, C., Fernandez, A., et al. (2009). Comparative investigation of $TiAlC$ (N), $TiCrAlC$ (N), and $CrAlC$ (N) coatings deposited by sputtering of MAX-phase $Ti_{2-x}Cr_xAlC$ targets. *Surf. Coatings Technol.* 203 (23), 3595–3609. doi:10.1016/j.surfcoat.2009.05.036
- Siebert, J. P., Bischoff, L., Lepple, M., Zintler, A., Molina-Luna, L., Wiedwald, U., et al. (2019). Sol-gel-based synthesis and enhanced processability of MAX phase Cr_2GaC . *J. Mater. Chem. C* 7 (20), 6034–6040. doi:10.1039/c9tc01416k
- Soundiraraju, B., Raghavan, R., and George, B. K. (2020). Chromium carbide nanosheets prepared by selective etching of aluminum from Cr_2AlC for hydrazine detection. *ACS Appl. Nano Mater.* 3 (11), 11007–11016. doi:10.1021/acsnm.0c02230
- Spanier, J. E., Gupta, S., Amer, M. S., and Barsoum, M. W. (2005). Vibrational behavior of the Mn phases from first-order Raman scattering Raman scattering (M= Ti, V, Cr, Ti, V, Cr, A= Si, X= C, N). *Phys. Rev. B Phys. Rev. B* 71, 012103.
- Sun, Z. M. (2011). Progress in research and development on MAX phases: a family of layered ternary compounds. *Int. Mater. Rev.* 56 (3), 143–166. doi:10.1179/1743280410y.0000000001
- Ta, Q. T. H., Tran, N. M., and Noh, J.-S. (2021). Pressureless manufacturing of Cr_2AlC compound and the temperature effect. *Mater. Manuf. Process.* 36 (2), 200–208. doi:10.1080/10426914.2020.1819547
- Tan, L., Guan, C., Tian, Y., Dang, P., Wang, S., Li, J., et al. (2019). Synthesis and tribological properties of ultrafine Cr_2AlC MAX phase. *Ceram. Soc. Jpn.* 127 (10), 754–760. doi:10.2109/jcersj2.18184

- Tian, W., Sun, Z., Du, Y., and Hashimoto, H. (2008). Synthesis reactions of Cr₂AlC from Cr–Al₄C₃–C by pulse discharge sintering. *Mater. Lett.* 62 (23), 3852–3855. doi:10.1016/j.matlet.2008.05.001
- Tunes, M. A., Httas, M. I., Kainz, C., Pogatscher, S., and Vishnyakov, V. M. (2021). Deviating from the pure MAX phase concept: radiation-tolerant nanostructured dual-phase Cr₂AlC. *Sci. Adv.* 7 (13), eabf6771. doi:10.1126/sciadv.abf6771
- Tzenov, N. V., and Barsoum, M. W. (2000). Synthesis and characterization of Ti₃AlC₂. *J. Am. Ceram. Soc.* 83 (4), 825–832. doi:10.1111/j.1151-2916.2000.tb01281.x
- Vishnyakov, V., Crisan, O., Dobrosz, P., and Colligon, J. S. (2014). Ion sputter-deposition and in-air crystallisation of Cr₂AlC films. *Vacuum* 100, 61–65. doi:10.1016/j.vacuum.2013.07.045
- Warsi, A.-Z., Aziz, F., Zulfiqar, S., Haider, S., Shakir, I., and Agboola, P. O. (2022). Synthesis, characterization, photocatalysis, and antibacterial study of WO₃, MXene and WO₃/MXene nanocomposite. *Nanomaterials* 12 (4), 713. doi:10.3390/nano12040713
- Wei, G.-L., Li, D.-Q., Zhuo, M.-N., Liao, Y.-S., Xie, Z.-Y., Guo, T.-L., et al. (2015). Organophosphorus flame retardants and plasticizers: sources, occurrence, toxicity and human exposure. *Environ. Pollut.* 196, 29–46. doi:10.1016/j.envpol.2014.09.012
- Yan, M., Duan, X., Zhang, Z., Liao, X., Zhang, X., Qiu, B., et al. (2017). Nanometre-scale 3D defects in Cr₂AlC thin films. *Sci. Rep.* 7 (1), 984. doi:10.1038/s41598-017-01196-3
- Yan, M., Duan, X., Zhang, Z., Liao, X., Zhang, X., Qiu, B., et al. (2019). Effect of ball milling treatment on the microstructures and properties of Cr₂AlC powders and hot pressed bulk ceramics. *J. Eur. Ceram. Soc.* 39 (16), 5140–5148. doi:10.1016/j.jeurceramsoc.2019.07.052
- Younas, M., Rizwan, M., Zubair, M., Inam, A., and Ali, S. (2021). Biological synthesis, characterization of three metal-based nanoparticles and their anticancer activities against hepatocellular carcinoma HepG2 cells. *Ecotoxicol. Environ. Saf.* 223, 112575. doi:10.1016/j.ecoenv.2021.112575
- Zamulaeva, E. I., Levashov, E. A., Skryleva, E. A., Sviridova, T. A., and Kiryukhantsev-Korneev, P. V. (2016). Conditions for formation of MAX phase Cr₂AlC in electrospark coatings deposited onto titanium alloy. *Surf. Coatings Technol.* 298, 15–23. doi:10.1016/j.surfcoat.2016.04.058
- Zamulaeva, E. I., Levashov, E. A., Sviridova, T. A., Shvyndina, N. V., and Petrzikh, M. I. (2013). Pulsed electrospark deposition of MAX phase Cr₂AlC based coatings on titanium alloy. *Surf. Coatings Technol.* 235, 454–460. doi:10.1016/j.surfcoat.2013.08.002
- Zhang, p., Yan, S., Li, C., Ding, Y., He, J., and Yin, F. (2019). Synthesis and characterization of MAX phase Cr₂AlC based composite coatings by plasma spraying and post annealing. *J. Eur. Ceram. Soc.* 39 (16), 5132–5139. doi:10.1016/j.jeurceramsoc.2019.08.039
- Zhang, Y., Wen, J., Zhang, L., Lu, H., Guo, Y., Ma, X., et al. (2021). High antioxidant lamellar structure Cr₂AlC: dielectric and microwave absorption properties in X band. *J. Alloys Compd.* 860, 157896. doi:10.1016/j.jallcom.2020.157896